AD-A171 461 SUPERSONIC FLOW OVER CYLINDRICAL AFTERBODIES WITH BASE BLEED(U) ARMY BALLISTIC RESEARCH LAB ABERDEEN PROVING GROUND MD J SAHU JUN 86 BRL-TR-2742 SBI-AD-F300 793 1/1

UNCLASSIFIED F/G 20/4 NL

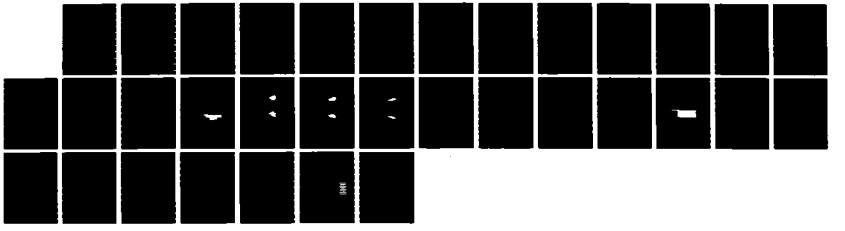

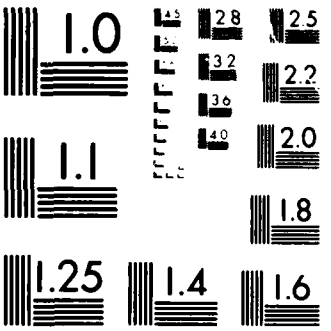

US ARMY MATERIEL COMMAND

TECHNICAL REPORT BRL-TR-2742

SUPERSONIC FLOW OVER CYLINDRICAL AFTERBODIES WITH BASE BLEED

Jubaraj Sahu

June 1986

US ARMY BALLISTIC RESEARCH LABORATORY
ABERDEEN PROVING GROUND, MARYLAND

Destroy this report when it is no longer needed.
Do not return it to the originator.

Additional copies of this report may be obtained from the National Technical Information Service, U. S. Department of Commerce, Springfield, Virginia 22161.

The findings in this report are not to be construed as an official Department of the Army position, unless so designated by other authorized documents.

The use of trade names or manufacturers' names in this report does not constitute indorsement of any commercial product.

UNCLASSIFIED
SECURITY CLASSIFICATION OF THIS PAGE

REPORT DOCUMENTATION PAGE

Form Approved
OMB No 0704-0188
Exp Date Jun 30, 1986

1a REPORT SECURITY CLASSIFICATION UNCLASSIFIED	1b RESTRICTIVE MARKINGS
2a SECURITY CLASSIFICATION AUTHORITY	3 DISTRIBUTION / AVAILABILITY OF REPORT Approved for public release, distribution unlimited.
2b DECLASSIFICATION / DOWNGRADING SCHEDULE	
4 PERFORMING ORGANIZATION REPORT NUMBER(S) Technical Report BRL-TR-2742	5 MONITORING ORGANIZATION REPORT NUMBER(S)
6a NAME OF PERFORMING ORGANIZATION U.S. Army Ballistic Research Laboratory 6b OFFICE SYMBOL (If applicable) SLCBR-LF	7a NAME OF MONITORING ORGANIZATION
6c ADDRESS (City, State, and ZIP Code) Aberdeen Proving Ground, Maryland 21005-5066	7b ADDRESS (City, State, and ZIP Code)
8a NAME OF FUNDING / SPONSORING ORGANIZATION 8b OFFICE SYMBOL (If applicable)	9 PROCUREMENT INSTRUMENT IDENTIFICATION NUMBER
8c ADDRESS (City, State, and ZIP Code)	10 SOURCE OF FUNDING NUMBERS PROGRAM ELEMENT NO: RDT&E PROJECT NO: 1L161102 TASK NO: AF43 WORK UNIT ACCESSION NO:

11 TITLE (Include Security Classification)
SUPERSONIC FLOW OVER CYLINDRICAL AFTERBODIES WITH BASE BLEED

12 PERSONAL AUTHOR(S)
SAHU, JUBARAJ

13a TYPE OF REPORT	13b TIME COVERED	14 DATE OF REPORT (Year, Month, Day)	15 PAGE COUNT
Final	FROM _____ TO _____	June 1986	32

16 SUPPLEMENTARY NOTATION

17 COSATI CODES			18 SUBJECT TERMS (Continue on reverse if necessary and identify by block number)
FIELD	GROUP	SUB-GROUP	Base Flow; Base Bleed; Supersonic Flow; Navier-Stokes; Cylindrical Afterbodies; Base Drag
01	01		

19 ABSTRACT (Continue on reverse if necessary and identify by block number)
Computations of supersonic flow over two cylindrical afterbodies have been made using a thin-layer Navier-Stokes base flow code. The capability to compute the base flow with base bleed at supersonic speeds has been developed and used to show the effect of mass injection on the base pressure or base drag. Solutions have been obtained for a projectile and a missile configuration having cylindrical afterbodies. Numerical results show the effect of base bleed on the near wake flow field. The rise in base pressure or reduction in base drag has been clearly predicted for various mass injection rates and comparison with experimental data shows generally good agreement.

20 DISTRIBUTION / AVAILABILITY OF ABSTRACT	21 ABSTRACT SECURITY CLASSIFICATION
☒ UNCLASSIFIED/UNLIMITED ☐ SAME AS RPT ☐ DTIC USERS	UNCLASSIFIED
22a NAME OF RESPONSIBLE INDIVIDUAL Jubaraj Sahu	22b TELEPHONE (Include Area Code) (301) 278-3707 22c OFFICE SYMBOL SLCBR-LF-R

DD FORM 1473, 84 MAR — 83 APR edition may be used until exhausted. All other editions are obsolete.

SECURITY CLASSIFICATION OF THIS PAGE
UNCLASSIFIED

TABLE OF CONTENTS

LIST OF ILLUSTRATIONS

I. INTRODUCTION

One of the most important aerodynamic performance characteristics for shell is the total drag. The total drag for projectiles can be divided into three components: (1) pressure drag (excluding the base), (2) viscous (skin friction) drag, and (3) base drag. The base drag is a major contributor to the total drag and can be as much as 50-60% of the total drag. It is, thus, important to minimize this part of the drag.

An effective means of reducing the base drag is by base bleed. In this method, a relatively small quantity of low velocity gas is injected into the dead air region immediately behind the base. This changes the structure of the flow field in the base region (See Figure 1) which results in an increase in the base pressure or reduction in the base drag. As mass flow rate of gas injected into the base region is increased from zero, the base pressure first increases (See Figure 2) until a maximum is reached. With further increase in mass injection, the base pressure falls to a minimum and then rises again. The 'base bleed' region is the first part of this curve up to the maximum which corresponds to very small rates of gas injection (of the order of a few percent).

The drag reduction due to base bleed at supersonic speeds is of practical importance. The concept of mass injection at the base has received considerable interest in the past and an excellent review is reported by Murthy et al.[1] As reported in Reference 1, there is a lack of detailed experimental measurements of the base flow phenomena with or without mass injection. Supersonic flow over cylindrical afterbodies with gas injection has been experimentally studied by Bowman and Clayden.[2] Their results showed the effect of mass injection on the base pressure for a range of Mach numbers between 1.5 and 3.0. For low Mach numbers ($M \approx 1.5$), an increase in base pressure was obtained with increasing mass flow rate of gas injection. For higher Mach numbers, the typical pattern of the effect of gas injection on the base pressure shown in Figure 2 was obtained. The effect of heating the injected gas results in a further but relatively small increase in base pressure or decrease in base drag.[3] More recently, Schilling[4] performed an experimental study to investigate base bleed effect on cylindrical and boattailed afterbodies where primary emphasis was to assess the effect of the tail fins on the

---

1. *Murthy, S.N.B., (Ed.), Progress in Astronautics and Aeronautics: Aerodynamics of Base Combustion," Vol. 40, AIAA, New York, 1976.*

2. *Bowman, J.E. and Clayden, W.A., "Cylindrical Afterbodies in Supersonic Flow with Gas Ejection," AIAA Journal, Vol. 5, No. 8, August 1967, pp. 1524-1525.*

3. *Clayden, W.A. and Bowman, J.E., "Cylindrical Afterbodies at $M_\infty = 2$ with Hot Gas Ejection," AIAA Journal, Vol. 6, No. 12, December 1968, pp. 2429-2431.*

4. *Schilling, H. "Experimental Investigation on the Base-Bleed-Effect for Body-Tail-Combinations," Proceedings of the 8th International Symposium on Ballistics, Amsterdam, Holland, 1984.*

effectiveness of base bleed. These experiments showed a strong interaction between the fins and the base region flow and the negative effect it has on the base drag reduction. Questions regarding the difference between hot gas injection and cold gas injection, the effect of base bleed on stability characteristics, the effect of spin on the base bleed effect and base combustion still remain to be answered. Very few semi-empirical methods are available to predict the reduction in base drag due to base bleed. One such method has been developed by Hellgren[5] in Sweden. An attempt has been made in this method to take into account the variation of burning conditions in the base bleed motor. Uncertainty in the base drag coefficient and also in the effect of spin on the burning base bleed propellant exists in this method. The application of sophisticated computational techniques to the practical base bleed problem is in its infancy. Limited computational work has been reported by Sullins et al[6] which dealt with the numerical computation of base region flow with parallel gas injection using two-dimensional Navier-Stokes equations. Recently, a new numerical capability has been developed by Sahu et al[7] to compute the base region flow using Azimuthal-Invariant thin-layer Navier-Stokes equations. Since the entire projectile flow field was computed, it was possible to obtain the total drag at transonic speeds. An attempt was also made to include the base injection at transonic speeds using crude base boundary conditions although the primary interest of the base bleed concept is in the supersonic speed regime.

This paper describes a computational investigation of the effect of centered base bleed on the base region flow field and on the base pressure at supersonic speeds using basically the same numerical procedure of Reference 7. A new interactive base bleed boundary condition procedure has been developed to determine the bleed exit boundary conditions. The resulting numerical capability is used to compute supersonic flow over two axisymmetric cylindrical afterbodies with gas injection and the computed results are compared to experiment. This is a first step towards obtaining a capability to predict the effect of base bleed (including combustion in the base region) on the aerodynamics of Army projectiles.

---

5. *Hellgren, R.V., "Range Calculation for Base Bleed Propellants," Proceedings of the 6th International Symposium on Ballistics, Orlando, Florida, 1981.*

6. *Sullins, G.A., Anderson, J.D., and Drummond, J.P., "Numerical Investigation of Supersonic Base Flow with Parallel Injection," AIAA Paper No. 82-1001, June 1982.*

7. *Sahu, J., Nietubicz, C.J., and Steger, J.L., "Navier-Stokes Computations of Projectile Base Flow with and without Base Injection," US Army Ballistic Research Laboratory, Aberdeen Proving Ground, Maryland, ARBRL-TR-02532, November 1983. (AD A135739) (Also see AIAA Journal, Vol. 23, No. 9, September 1985, pp. 1348-1355)*

II. COMPUTATIONAL TECHNIQUE

The Azimuthal Invariant (or Generalized Axisymmetric) thin-layer Navier-Stokes equations for general spatial coordinates ξ, η, ζ can be written as:[8]

$$\partial_\tau \hat{q} + \partial_\xi \hat{E} + \partial_\zeta \hat{G} + \hat{H} = Re^{-1} \partial_\zeta \hat{S} \tag{1}$$

where $\xi = \xi(x,y,z,t)$ is the longitudinal coordinate

$\eta = \eta(y,z,t)$ is the circumferential coordinate

$\zeta = \zeta(x,y,z,t)$ is the near normal coordinate

$\tau = t$ is the time

and

$$\hat{q} = J^{-1} \begin{bmatrix} \rho \\ \rho u \\ \rho v \\ \rho w \\ e \end{bmatrix} , \quad \hat{E} = J^{-1} \begin{bmatrix} \rho U \\ \rho uU + \xi_x p \\ \rho vU + \xi_y p \\ \rho wU + \xi_z p \\ (e+p)U - \xi_t p \end{bmatrix} , \quad \hat{G} = J^{-1} \begin{bmatrix} \rho W \\ \rho uW + \zeta_x p \\ \rho vW + \zeta_y p \\ \rho wW + \zeta_z p \\ (e+p)W - \zeta_t p \end{bmatrix} ,$$

$$\hat{H} = J^{-1} \begin{bmatrix} 0 \\ 0 \\ \rho V[R_\xi(U-\xi_t) + R_\zeta(W-\zeta_t)] \\ -\rho VR(V-\eta_t) - p/R \\ 0 \end{bmatrix}$$

---

8. *Nietubicz, C.J., Pulliam, T.H., and Steger, J.L., "Numerical Solution of the Azimuthal-Invariant Navier-Stokes Equations," US Army Ballistic Research Laboratory, Aberdeen Proving Ground, Maryland, ARBLR-TR-02227, March 1980. (AD A085716) (Also see AIAA Journal, Vol. 18, No. 12, December 1980, pp. 1411-1412)*

$$\hat{S} = \begin{bmatrix} 0 \\ \mu(\zeta_x^2 + \zeta_y^2 + \zeta_z^2)u_\zeta + (\mu/3)(\zeta_x u_\zeta + \zeta_y v_\zeta + \zeta_z w_\zeta)\zeta_x \\ \mu(\zeta_x^2 + \zeta_y^2 + \zeta_x^2)v_\zeta + (\mu/3)(\zeta_x u_\zeta + \zeta_y v_\zeta + \zeta_z w_\zeta)\zeta_y \\ \mu(\zeta_x^2 + \zeta_y^2 + \zeta_z^2)w_\zeta + (\mu/3)(\zeta_x u_\zeta + \zeta_y v_\zeta + \zeta_z w_\zeta)\zeta_z \\ \{(\zeta_x^2 + \zeta_y^2 + \zeta_y^2)[(\mu/2)(u^2 + v^2 + w^2)_\zeta + \kappa Pr^{-1}(\gamma-1)^{-1}(a^2)_\zeta] \\ \quad + (\mu/3)(\zeta_x u + \zeta_y v + \zeta_z w)(\zeta_x y_\zeta + \zeta_y v_\zeta + \zeta_z w_\zeta)\} \end{bmatrix}$$

The velocities

$$\begin{aligned} U &= \xi_t + \xi_x u + \xi_y v + \xi_z w \\ V &= \eta_t + \eta_x u + \eta_y v + \eta_z w \\ W &= \zeta_t + \zeta_x u + \zeta_y v + \zeta_z w \end{aligned} \tag{2}$$

represent the contravariant velocity components.

The Cartesian velocity components (u, v, w) are nondimensionalized with respect to a_∞ (free stream speed of sound). The density (ρ) is referenced to ρ_∞ and total energy (e) to $\rho_\infty a_\infty^2$. The local pressure is determined using the equation of state,

$$P = (\gamma - 1)[e - 0.5\rho(u^2 + V^2 + w^2)] \tag{3}$$

where γ is the ratio of specific heats.

In Equation (1), axisymmetric flow assumptions have been made which result in the source term, $\hat{H}$. The details of how this is obtained can be found in Reference (8) and are not discussed here. Equation (1) contains only two spatial derivatives. However, it retains all three momentum equations and allows a degree of generality over the standard axisymmetric equations. In particular, the circumferential velocity is not assumed to be zero thus allowing computations for spinning projectiles to be accomplished. This is especially important to study the effect of spin on the base bleed effect.

The numerical algorithm used is the Beam-Warming fully implicit, approximately factored finite difference scheme. The algorithm can be first or

second order accurate in time and second or fourth order accurate in space. Since the interest is only in the steady-state solution, Equation (1) is solved in an asymptotic fashion and first order accurate time differencing is used. The spatial accuracy is fourth order. Details of the algorithm are included in References 9-11.

To suppress high frequency components that appear in regions containing severe pressure gradients e.g., shocks or stagnation points, artificial dissipation terms are added. In the present application, a switching dissipation model is used which is a blend of second and fourth order dissipation terms. This is similiar to the model used by Pulliam[12] and uses a fourth order dissipation in smooth regions and switches to a second order dissipation in regions containing high pressure or density gradients. Incorporation of this dissipation model has resulted in the improvement of the quality of the results and has made the code more robust.

The numerical code used computes the full flow field over a projectile or a missile including the base region using a unique flow field segmentation procedure. An important advantage of this procedure lies in the preservation of the sharp corner at the base. The details of these can be found in Reference 7. For the computation of turbulent base flows, the two-layer algebraic Baldwin-Lomax turbulence model[13] is used. Higher order two-equation or more sophisticated turbulence models need to be considered for such flows in future.

III. BOUNDARY CONDITIONS

The no slip boundary condition for viscous flow is enforced by setting the contravariant velocities to zero i.e., $U = V = W = 0$ on the body surface. Inviscid boundary conditions are used at the base for the case of no gas injection. The pressure on the body surface is obtained by solving a combined momentum equation and density is extrapolated. First order extrapolation is used for both pressure and density at the base. Along the computational cut, the flow variables above and below are averaged to determine the conditions on

---

9. *Steger, J.L., "Implicit Finite Difference Simulation of Flow About Arbitrary Geometries with Application to Airfoils," AIAA Journal, Vol. 16, No. 4, July 1978, pp. 679-686.*

10. *Pulliam, T.H. and Steger, J.L., "On Implicit Finite-Difference Simulations of Three-Dimensional Flow," AIAA Journal, Vol. 18, No. 2, February 1980, pp. 159-167.*

11. *Beam, R. and Warming, R.F., "An Implicit Factored Scheme for the Compressible Navier-Stokes Equations," AIAA Paper No. 77-645, June 1977.*

12. *Pulliam, T.H., "Artificial Dissipation Models for the Euler Equations," AIAA Paper No. 85-0438, January 1985.*

13. *Baldwin, B.S. and Lomax, H., "Thin-Layer Approximation and Algebraic Model for Separated Turbulent Flows," AIAA Paper No. 78-257, 1978.*

the cut. A symmetry boundary condition is imposed on the centerline of the wake region with first order extrapolation for density and pressure. Free stream conditions are imposed on the outer boundary while extrapolated values of the variables are used at the downstream boundary.

For the base bleed case, boundary conditions along the base where gas is injected need to be modified. Here, a small amount of mass is injected into the near wake behind the center part of the base. The amount of gas injection is usually defined in terms of a mass injection parameter,

$$I = \frac{\dot{m}_j}{\rho_\infty u_\infty A_b}$$

where $\dot{m}_j$ is the mass flow at the bleed exit and A_b is the area at the base. At the bleed exit, the flow is subsonic and three quantities need to be specified. Total temperature is used at the exit along with an extrapolated value of static pressure. The static pressure at the exit is set equal to local pressure which is a characteristic of subsonic flows. Such extrapolated static pressure boundary conditions have been used in other numerical computations.[14] [15] In addition, the value of total pressure at the exit is needed to define all the boundary conditions. This is determined iteratively to satisfy the required mass injection parameter in the following manner. Knowing the total temperature (To_j) and mass injection parameter (I),

(a) assume total pressure, Po_j

(b) obtain P_j by extrapolation

(c) calculate Mach number, M_j using $Po_j/P_j = (1 + .2M_j^2)^{3.5}$

(d) compute ρ_j using $To_j/T_j = 1 + .2M_j^2$

(e) obtain the velocity $u_j = M_j a_j = M_j \sqrt{\gamma RT_j}$

(f) obtain the density ρ_j from the equation state, $P_j = \rho_j RT_j$

(g) compute $I = \rho_j u_j A_j / \rho_\infty u_\infty A_b$

---

14. *Shrewsbury, G.D., "Analysis of Circulation Control Airfoils Using an Implicit Navier-Stokes Solver," AIAA Paper NO. 85-0171, January 1985.*

15. *Drummond, J.P., "Numerical Study of a Ramjet Dump Combustor Flow Field," AIAA Paper No. 83-0421, January 1983.*

If the value of this I is not the desired value, then we go back to step (a) and continue the iteration process. This iteration procedure is repeated at each time step. The total pressure and the total temperature are assumed to be constant across the bleed exit.

IV. RESULTS

Computations of the flow field for two cylindrical afterbodies with base bleed have been made at supersonic speed and at zero angle of attack. The first set of computed results correspond in part to the experimental investigation on the base bleed effect by Schilling[4] whereas the second set of results are compared to the experimental measurements by Bowman et al[2] at the Royal Armament and Development Establishment (RARDE), England.

The experimental investigation by Schilling[4] was conducted at the Trisonic Wind Tunnel at the Deutsche Forschungs- und Versuchsanstalt für Luft- und Raumfahrt e. V. Köln (DFVLR) in West Germany for a missile configuration. A computational grid for this case showing the cylindrical afterbody region is shown in Figure 3. The full grid consisted of 156 points in the streamwise direction and 60 points in the normal direction. The grid has been adapted to the free shear layer as the solutions developed. The same grid was used for calculations with and without base bleed. The minimum grid spacing near the wall and in the free shear layer is .00002 caliber. Numerical computations were made at M_∞ = 1.7 and 2.5 at zero angle of attack.

Figure 4 shows the velocity vectors in the base region for the case of no gas injection whereas Figures 5 and 6 show the velocity vectors in the base region with gas injection for M_∞ = 2.5. In Figure 4, the recirculatory flow field in the near wake is clearly evident. The flow expands at the base and the reattachment point is about .75 caliber downstream of the base. The effect of gas injection at the base is shown in Figures 5 and 6 for mass injection rates I = .01 and .02, respectively. As shown in Figure 5 for I = .01, the separation bubble (for the no bleed case) has been displaced downstream and the size of the separation bubble has also been reduced. The flow field in the near wake has changed considerably. There are two stagnation points, one at X/D ≈ 15 and the other at X/D ≈ 15.4. This is a typical flow field pattern with base bleed at a low injection rate. As I is increased to .02, more mass is injected into the near wake and strongly affects the base region flow. As seen in Figure 6, the separation bubble that was displaced downstream somewhat at I = .01 has now been eliminated and the beginning of a small separation region near the base is seen. For this injection rate, the Mach number at the bleed exit approaches sonic value. Increasing the mass injection rate further gives Mach number unity at the bleed exit and results in the separation region in the near wake which resembles that of a jet effect.

Figure 7 shows the pressure distribution as a function of the longitudinal position over the cylindrical afterbody and along the upper shear layer in the wake region. The strong expansion at the base corner and the recompression waves downstream of the base corner are clearly seen for the zero base bleed case (I = 0). The pressure distribution for the base bleed case is presented in this figure for I = .01 and I = .02. As I increased to .01 from

zero, the expansions at the base and the recompression downstream of the base are both weakened. Increasing I further has the effect of weakening the waves even more.

The effect of mass injection on the base pressure and hence on base drag is of primary interest. Figure 8 shows the base drag as a function of the mass injection parameter for $M_\infty = 1.7$ and $\alpha = 0$. I = 0 corresponds to the case of no base bleed. As I is increased, the base pressure increases in this case and thus, base drag is reduced. This is true for both I = .01 and I = .02. The computed base drag is compared to the experimental data and as can be seen, the computed results are overpredicted by about 15%. The trend of base drag reduction seen experimentally however, has been clearly predicted by the computation. Additionally, the Mach number at the bleed exit is less than unity for all the mass injection rates considered here. The results for $M_\infty = 2.5$ is shown in Figure 9. Here the computed base drag is compared to experiment and excellent agreement is obtained for the zero bleed condition (I = 0). As the mass flow rate is increased to .01, base pressure increases and base drag is reduced. Comparison between the computation and the experiment again indicates 10-15% disagreement. The Mach number at the bleed exit (M_j) is approaching unity. As I is increased further to .02, M_j has reached the sonic condition and stays sonic as I is increased further. Here the trend reverses and a small increase in base drag is found. For I = .025, the computed base drag is in good agreement with the experiment.

Supersonic flow for another cylindrical afterbody with base bleed has been computed. Experimental measurements for this case have been made by Bowman et al[2] at RARDE, England. The model configuration was a projectile consisting of a two caliber ogive nose and a five caliber cylindrical afterbody. The bleed exit diameter was equal to 0.4 base diameter. Computations for this case have been made at two supersonic speeds. $M_\infty = 1.88$ and $M_\infty = 2.48$ at zero angle of attack. The computational grid used in this case for $M_\infty = 1.88$ is shown in Figure 10. The grid is adapted to the free shear layer in the wake and clustering of grid points is made near the base bleed exit. The number of grid points in the streamwise direction is 130 and 40 points are used in the normal direction. The qualitative results obtained in the base region with base bleed are similar to that discussed earlier. The effect of gas injection on the base pressure is discussed next.

Figures 11 and 12 show the ratio of base pressure to free stream static pressure as a function of the mass injection parameter, I for $M_\infty = 1.88$ and 2.48, respectively. As shown in Figure 11 for $M_\infty = 1.88$, base pressure increases as I is increased from zero. The agreement between the computed result and the experiment is very good. As I = .02 is approached, the base pressure ceases to rise according to the experimental data. Figure 12 shows the base pressure with and without base bleed between the computation and the experiment. As I is increased from zero to .01, both experiment and the computation show an increase in the base pressure and reasonably good agreement is obtained. Further increase in I clearly shows a large decrease in the base pressure as is seen in the experimental data. The computation doesn't show that much of a decrease in the base pressure although the trend is in

agreement with the experimental data. Also, the flow was assumed to be subsonic at the bleed exit in the computation; however, it is not clear what the exit condition was in the experiment. The comparison of the results for this case must be viewed in that light.

V. CONCLUDING REMARKS

A computational study has been made for base region flow over two cylindrical afterbodies with base bleed at supersonic speeds. An iterative boundary condition procedure was developed for the base bleed effect and was used to show the effect of base bleed on base pressure or base drag. The thin-layer form of the compressible Navier-Stokes equations was solved using a time-dependent implicit numerical algorithm. Numerical results show the qualitative effect of the mass injection on the near wake flow field. The expansions at the base and the recompression downstream of the base are weakened by the gas injection. For low supersonic Mach number $\simeq$ 1.75, base pressure rises smoothly as injected mass flow rate is increased. For the higher Mach number $\simeq$ 2.5, increase in base pressure or decrease in base drag is obtained at lower mass flow rates ($I = .01$). Further computational investigation is needed to include the effect of hot gas injection at the base. Future work will be directed towards obtaining a predictive capability to compute projectile base region flow with combustion for practical applications.

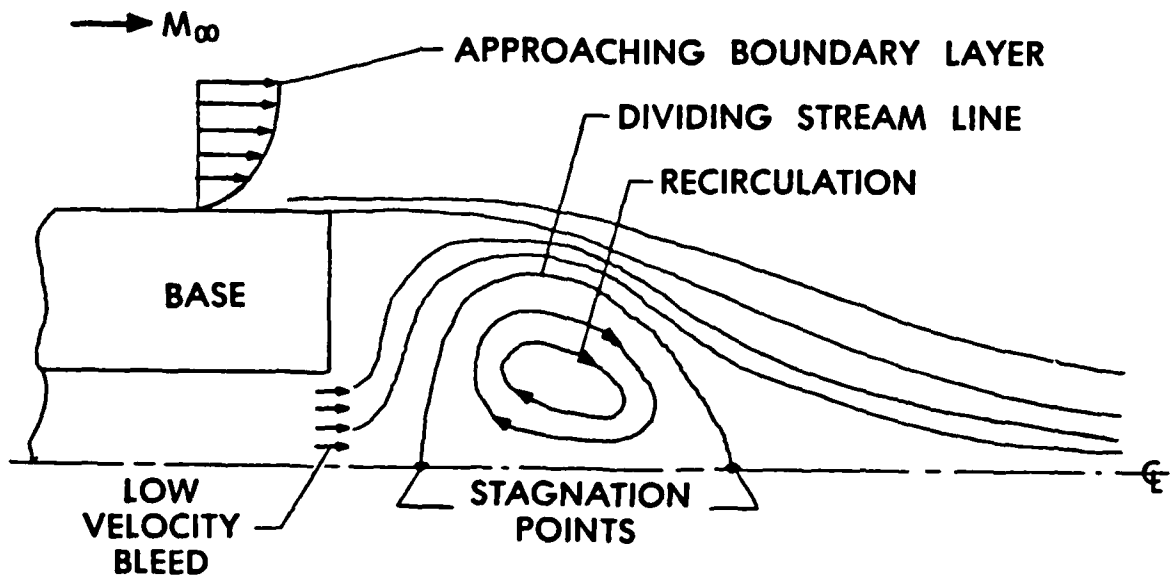

Figure 1. Schematic Illustration of Base Flow with Base Bleed

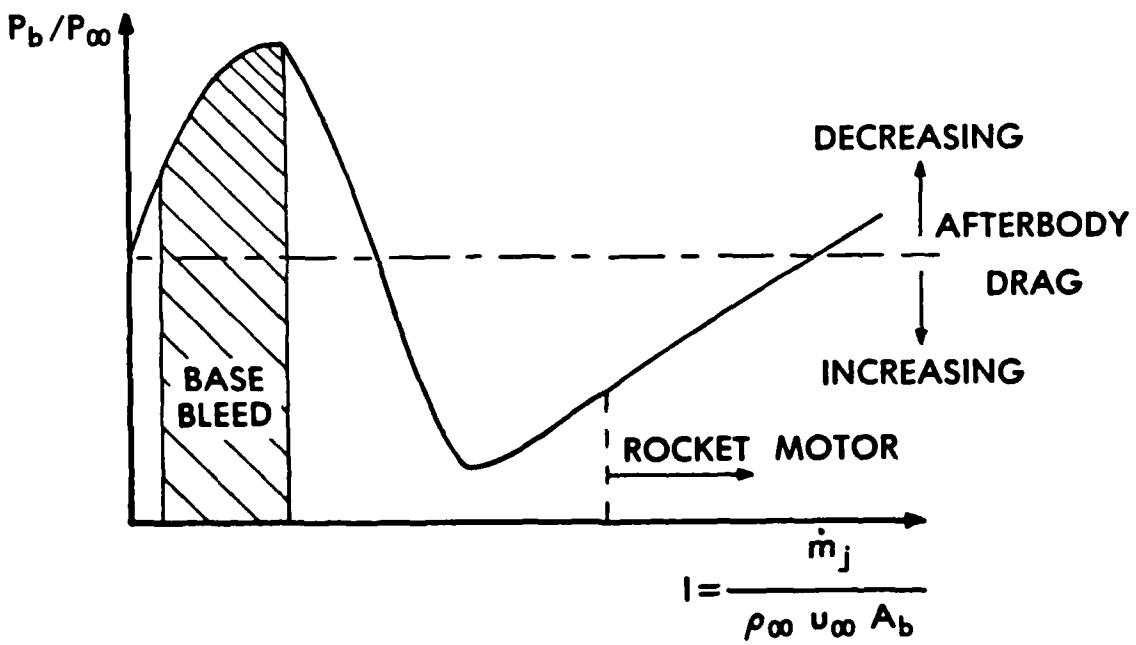

Figure 2. Base Pressure vs Mass Flow Rate of Injection

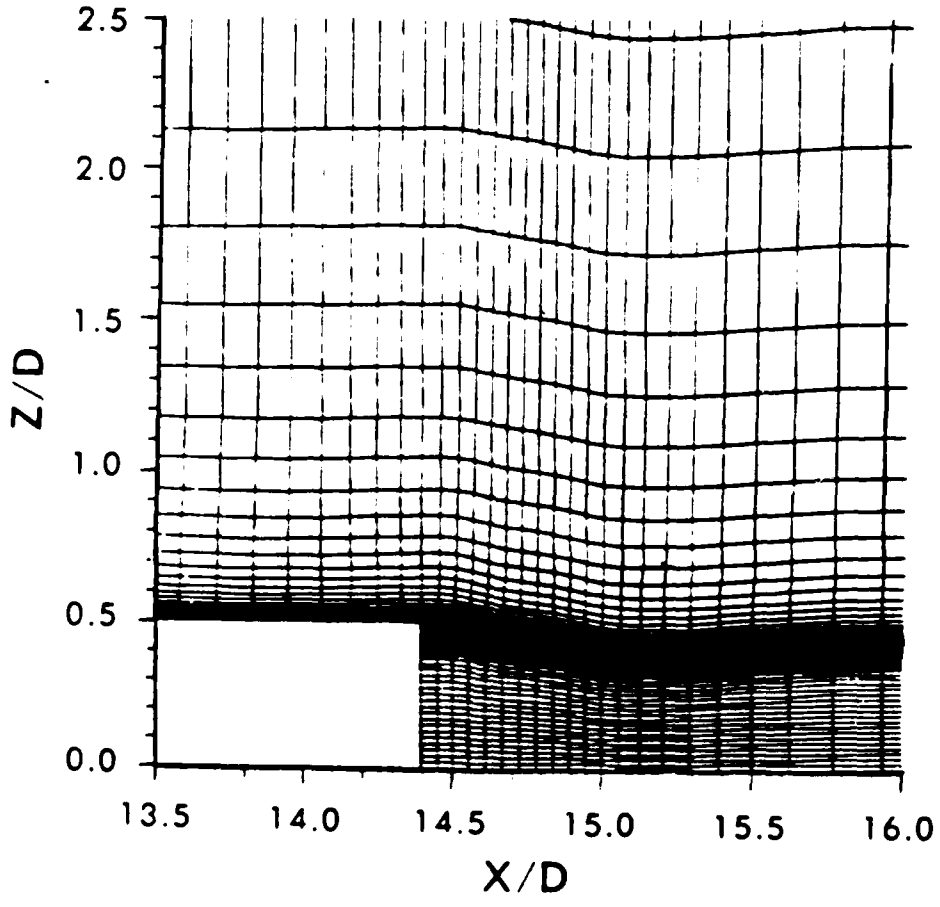

Figure 3. Adapted Grid in the Base Region, M_∞ = 2.5

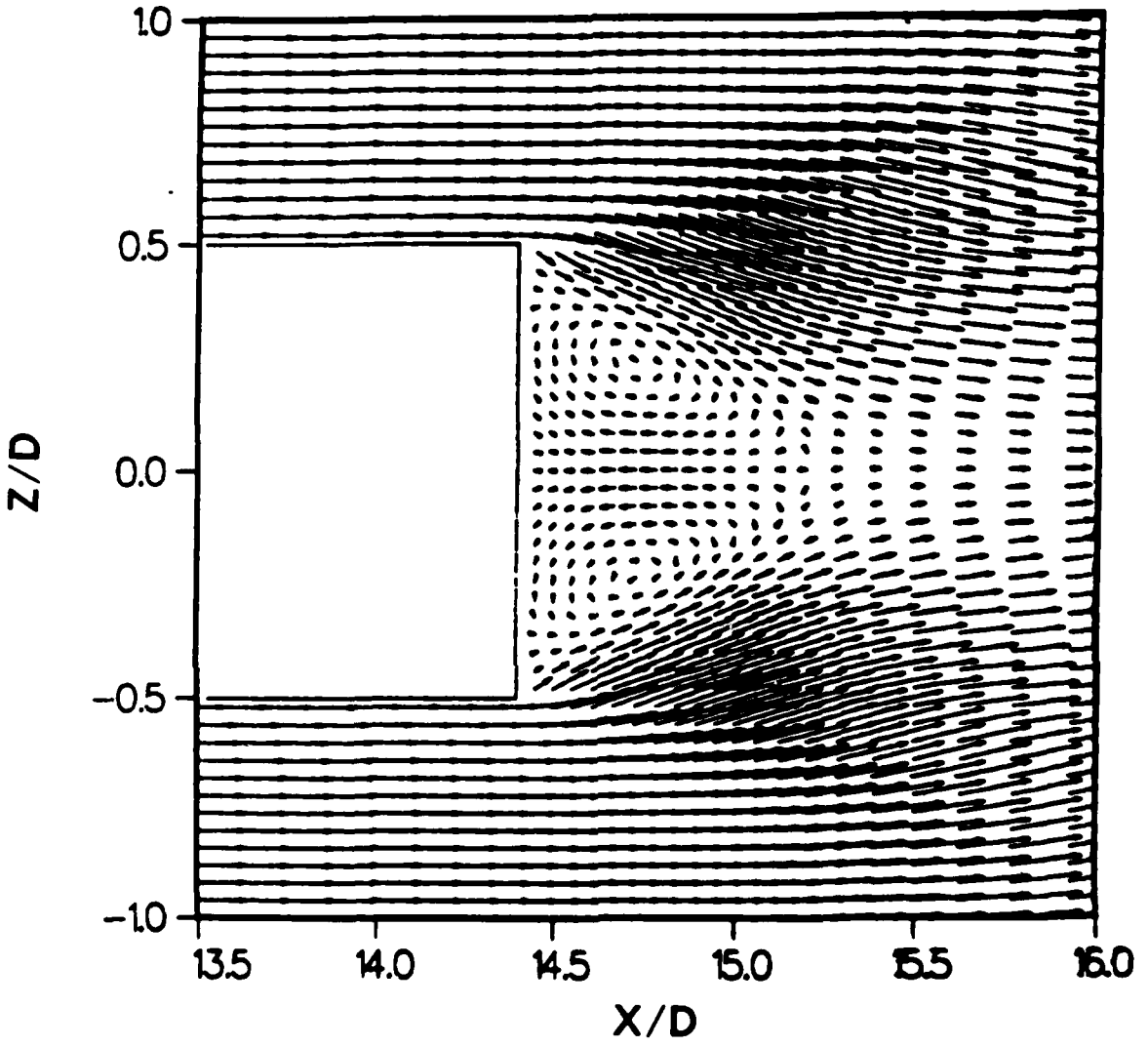

Figure 4. Velocity Vectors in the Base Region $M_\infty = 2.5$, $\alpha = 0$, $I = 0$

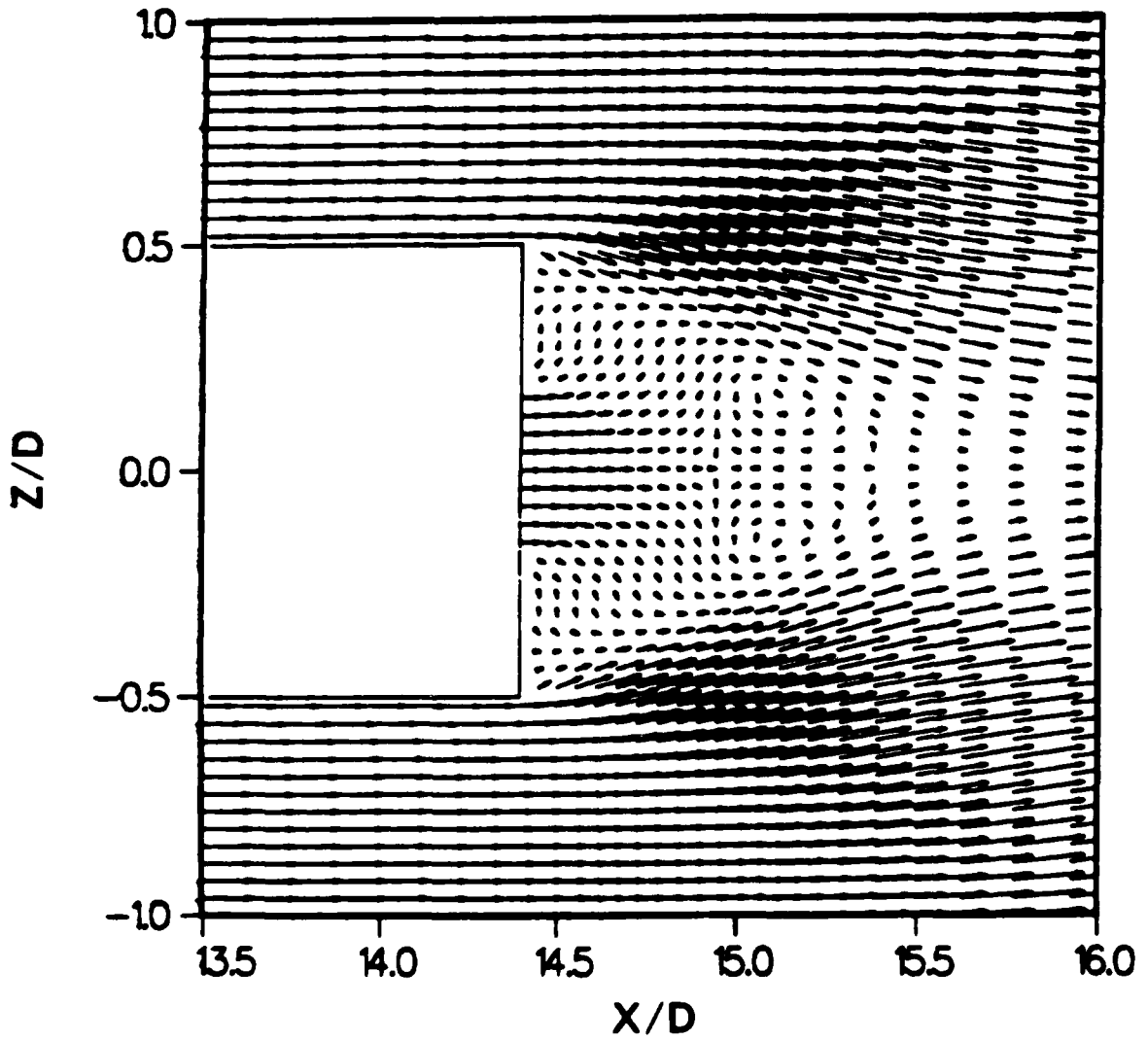

Figure 5. Velocity Vectors in the Base Region M_∞ = 2.5, α = 0, I = .01

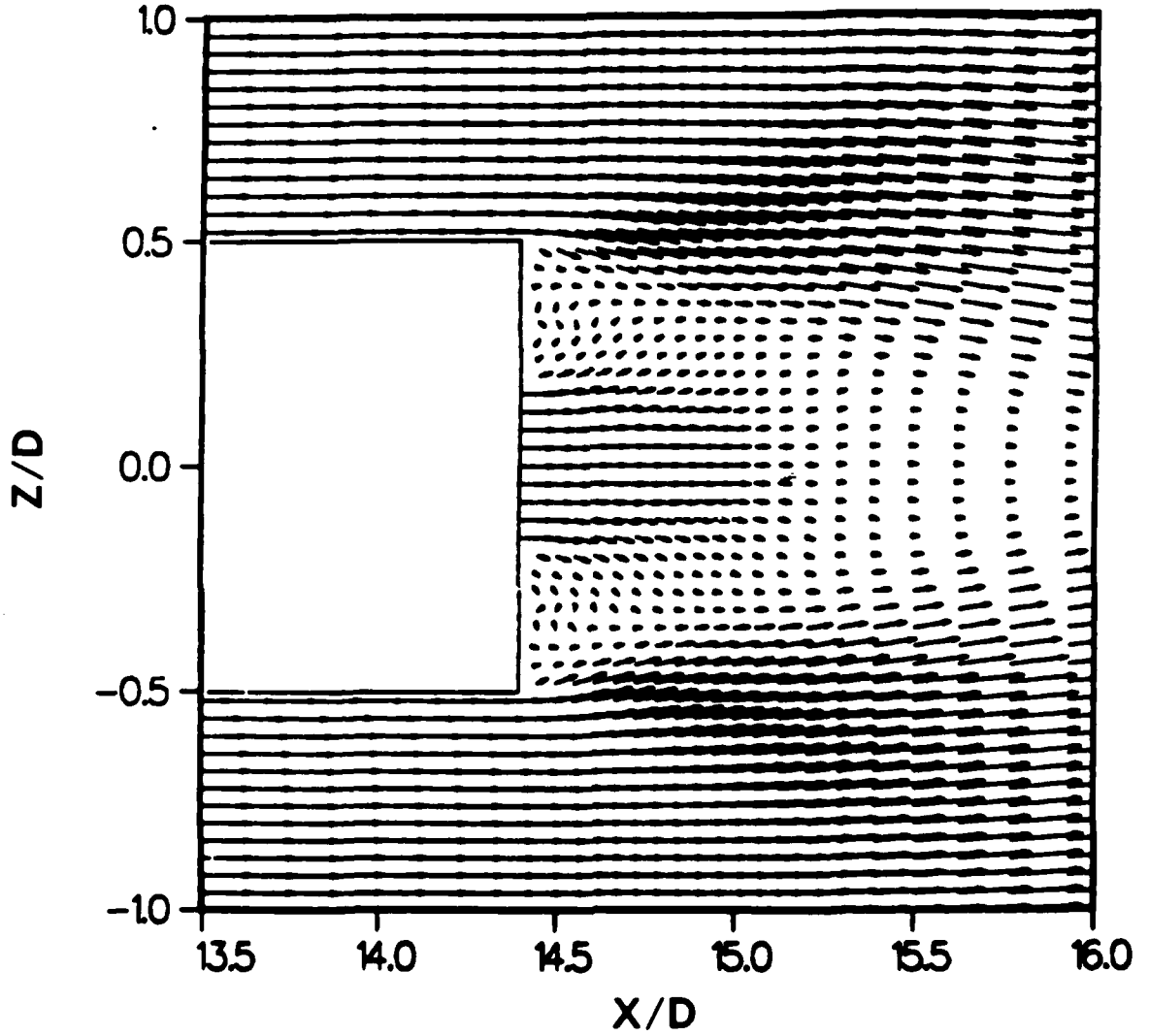

Figure 6. Velocity Vectors in the Base Region $M_\infty = 2.5$, $\alpha = 0$, $I = .02$

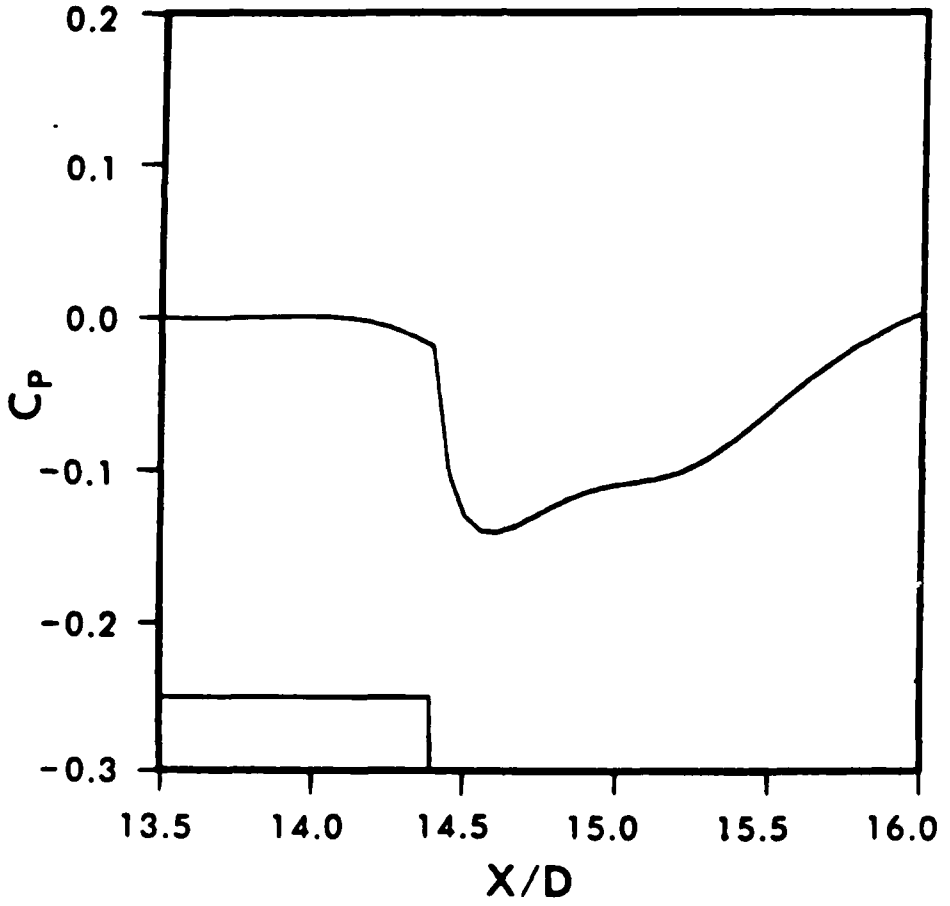

Figure 7a. Longitudinal Pressure Distribution, M_∞ = 2.5, α = 0, I = 0

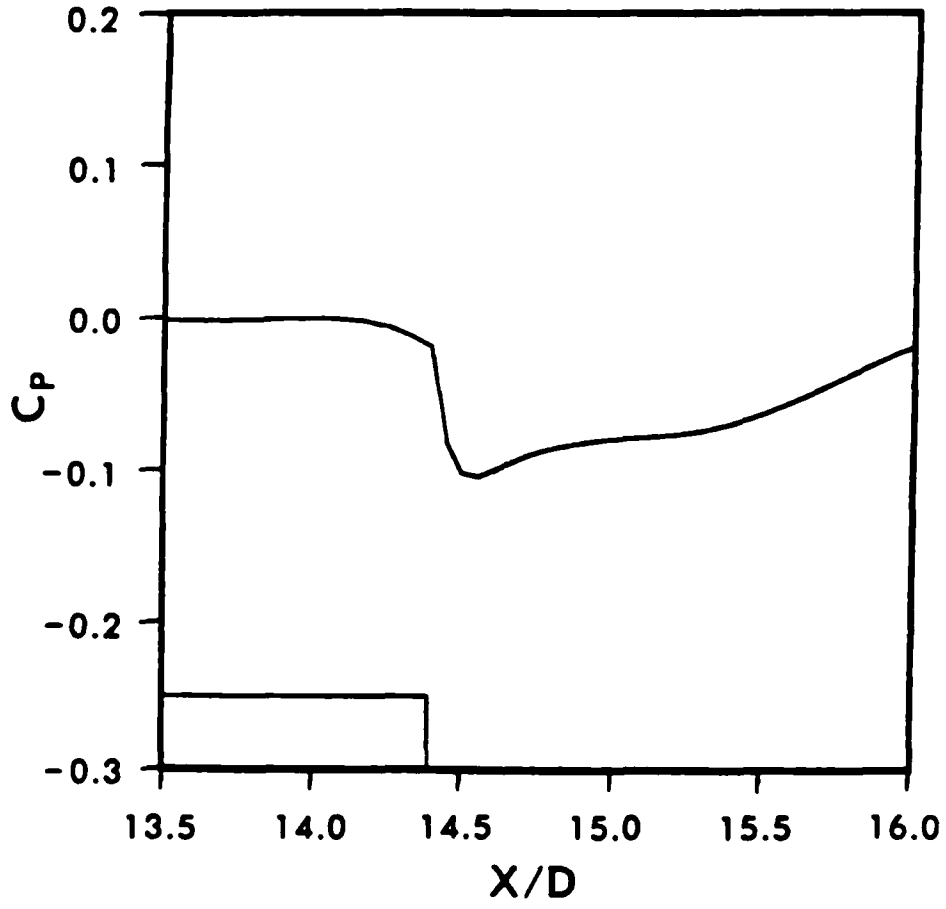

Figure 7b. Longitudinal Pressure Distribution, M_∞ = 2.5, α = 0, I = .01

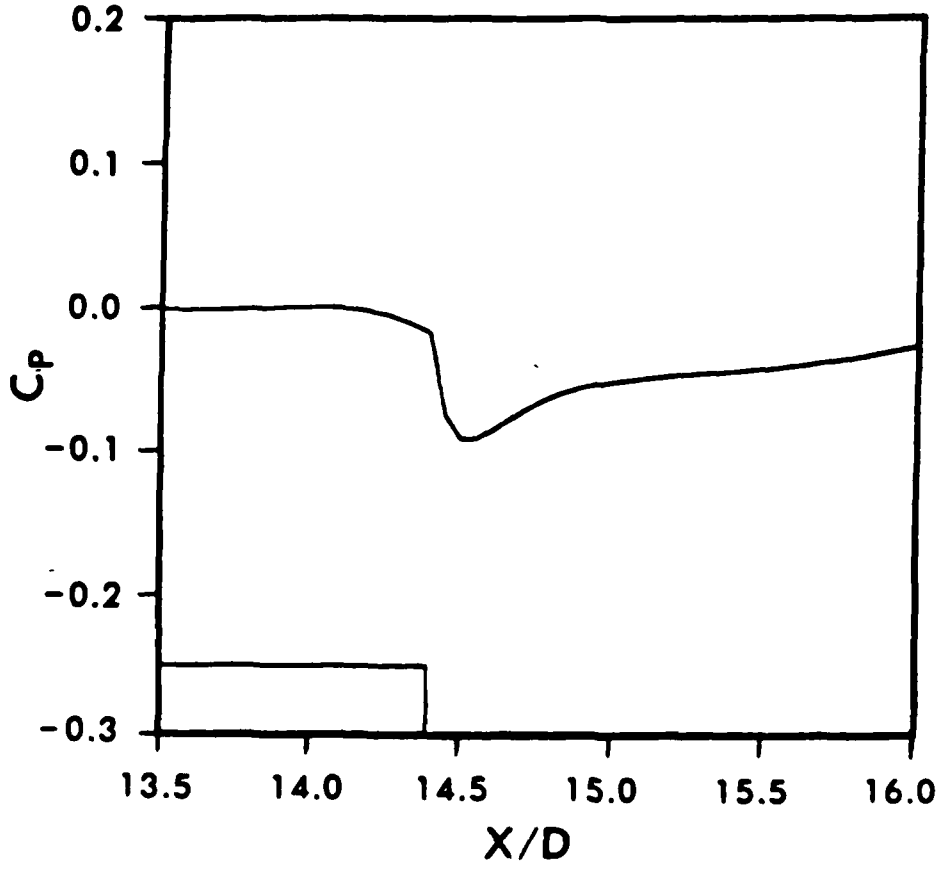

Figure 7c. Longitudinal Pressure Distribution, M_∞ = 2.5, α = 0, I = .02

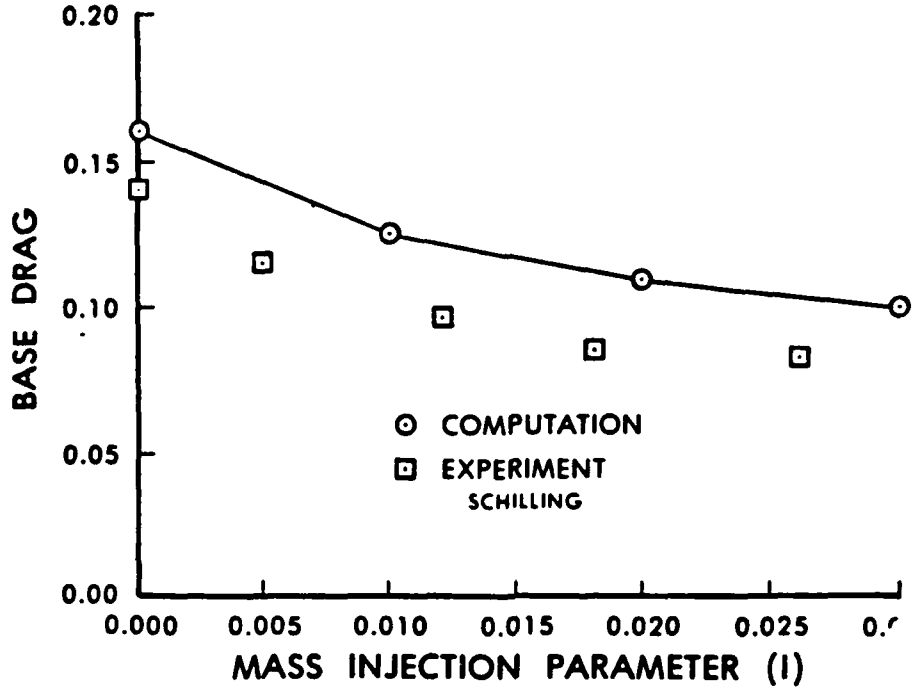

Figure 8. Base Drag vs Mass Injection Parameter, $M_\infty = 1.7$, $\alpha = 0$

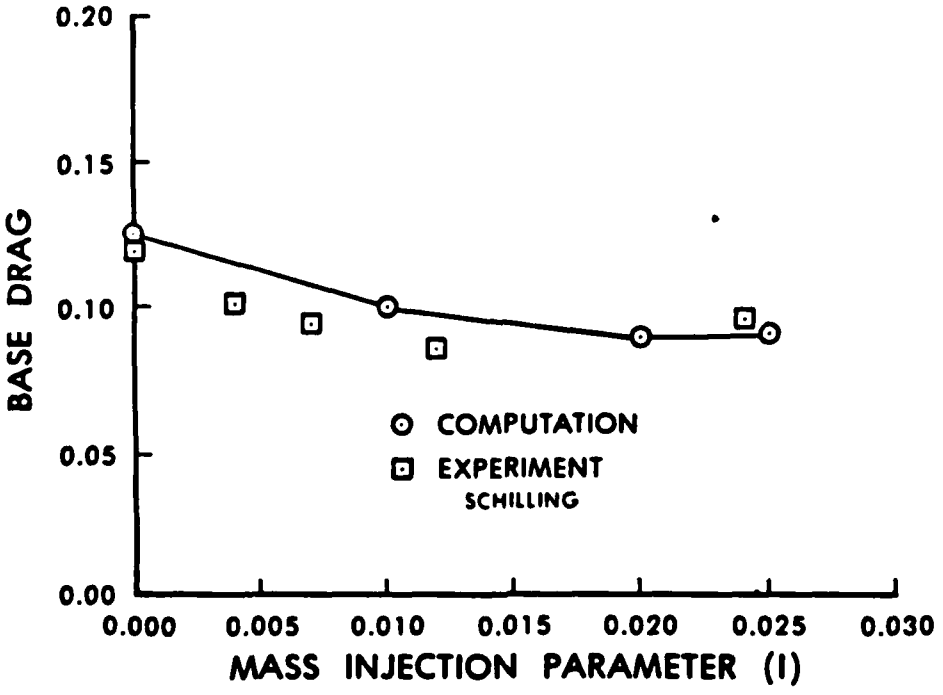

Figure 9. Base Drag vs Mass Injection Parameter $M_\infty = 2.5$, $\alpha = 0$

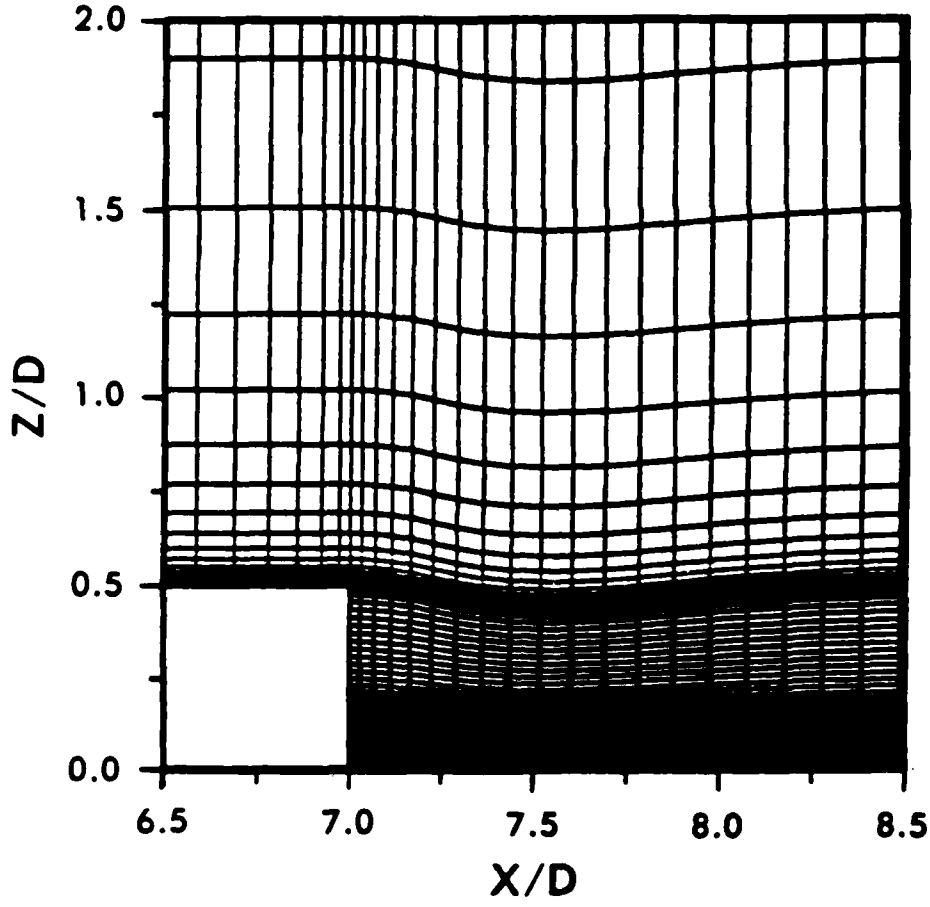

Figure 10. Adapted Grid in the Base Region for RARDE Case, $M_\infty = 1.88$, $\alpha = 0$

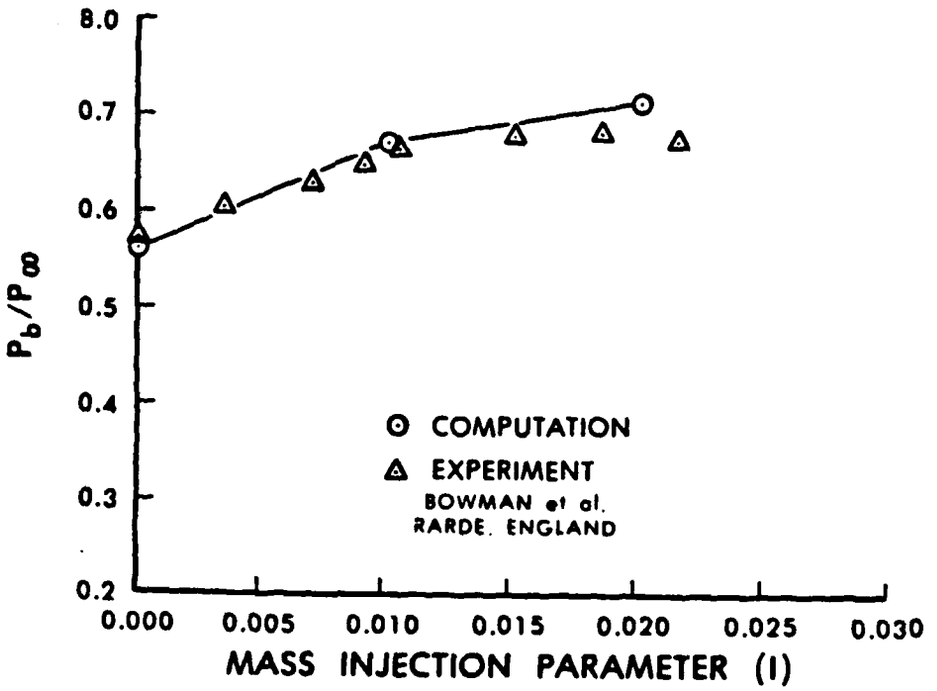

Figure 11. Base Pressure vs Mass Injection Parameter, $M_\infty = 1.88$, $\alpha = 0$

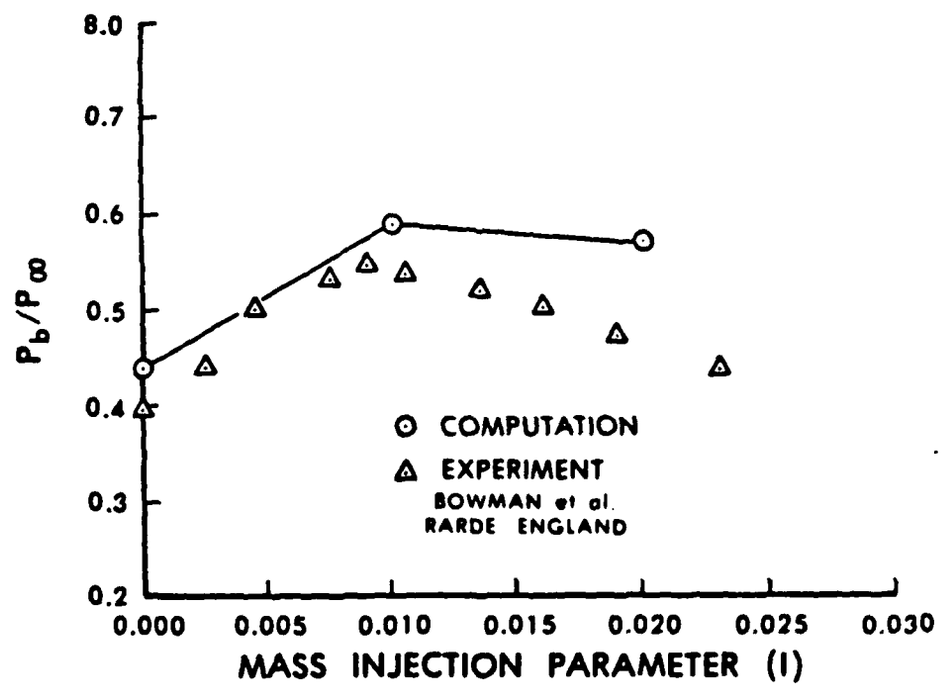

Figure 12. Base Pressure vs Mass Injection Parameter, $M_\infty = 2.48$, $\alpha = 0$

REFERENCES

1. Murthy, S.N.B., (Ed.), "Progress in Astronautics and Aeronautics: Aerodynamics of Base Combustion," Vol. 40, AIAA, New York, 1976.

2. Bowman, J.E. and Clayden, W.A., "Cylindrical Afterbodies in Supersonic Flow with Gas Ejection," AIAA Journal, Vol. 5, No. 8, August 1967, pp. 1524-1525.

7

3. Clayden, W.A. and Bowman, J.E. "Cylindrical Afterbodies at $M_\infty = 2$ with Hot Gas Ejection," AIAA Journal, Vol. 6, No. 12, December 1968, pp. 2429-2431.

4. Schilling, H., "Experimental Investigation on the Base-Bleed-Effect for Body-Tail-Combinations," Proceedings of the 8th International Symposium on Ballistics, Amsterdam, Holland, 1984.

5. Hellgren, R.V., "Range Calculation for Base bleed Propellants," Proceedings of the 6th International Symposium on Ballistics, Orlando, Florida, 1981.

6. Sullins, G.A., Anderson, J.D., and Drummond, J.P., "Numerical Investigation of Supersonic Base Flow with Parallel Injection," AIAA Paper No. 82-1001, June 1982.

7. Sahu, J., Nietubicz, C.J., and Steger, J.L., "Navier-Stokes Computations of Projectile Base Flow with and without Base Injection," US Army Ballistic Research Laboratory, Aberdeen Proving Ground, Maryland, ARBRL-TR-02532, November 1983. (AD A135738) (Also see AIAA Journal, Vol. 23, No. 9, September 1985, pjp. 1348-1355)

8. Nietubicz, C.J., Pulliam, T.H., and Steger, J.L., "Numerical Solution of the Azimuthal-Invariant Navier-Stokes Equations," US Army Ballistic Research Laboratory, Aberdeen Proving Ground, Maryland, ARBRL-TR-02227, March 1980. (AD A085716) (Also see AIAA Journal, Vol. 18, No. 12, December 1980, pp. 1411-1412)

9. Steger, J.L., "Implicit Finite Difference Simulation of Flow About Arbitrary Geometries with Application to Airfoils," AIAA Journal, Vol. 16, No. 4, July 1978, pp. 679-686.

10. Pulliam, T.H. and Steger, J.L., "On Implicit Finite-Difference Simulations of Three-Dimensional Flow," AIAA Journal, Vol. 18, No. 2, February 1980, pp. 159-167.

11. Beam, R. and Warming, R.F., "An Implicit Factored Scheme for the Compressible Navier-Stokes Equations," AIAA Paper No. 77-645, June 1977.

12. Pulliam, T.H., "Artificial Dissipation Models for the Euler Equations," AIAA Paper No. 85-0438, January 1985.

13. Baldwin, B.S. and Lomax, H., "Thin-Layer Approximation and Algebraic Model for Separated Turbulent Flows," AIAA Paper No. 78-257, 1978.

14. Shrewsbury, G.D., "Analysis of Circulation Control Airfoils Using an Implicit Navier-Stokes Solver," AIAA Paper No. 85-0171, January 1985.

15. Drummond, J.P., "Numerical Study of a Ramjet Dump Combustor Flow Field," AIAA Paper No. 83-0421, January 1983.

DISTRIBUTION LIST

No. of Copies	Organization
12	Administrator Defense Technical Info Center ATTN: DTIC-DDA Cameron Station Alexandria, VA 22304-6145
1	HQDA DAMA-ART-M Washington, DC 20310
1	Commander US Army Materiel Command ATTN: AMCDRA-ST 5001 Eisenhower Avenue Alexandria, VA 22333-0001
6	Commander Armament RD&E Center US Army AMCCOM ATTN: SMCAR-TDC SMCAR-TSS SMCAR-LCA-F Mr. D. Mertz Mr. A. Loeb Mr. H. Hudgins Mr. E. Friedman Dover, NJ 07801-5001
1	Commander US Army Armament, Munitions & and Chemical Command ATTN: SMCAR-ESP-L Rock Island, IL 61299
1	Director Benet Weapons Laboratory Armament RD&E Center US Army AMCCOM ATTN: SMCAR-LCB-TL Watervliet, NY 12189
1	Commander US Army Aviation Research and Development Command ATTN: AMSAV-E 4300 Goodfellow Blvd. St. Louis, MO 63120
1	Director US Army Air Mobility Research and Development Command Ames Research Center Moffett Field, CA 94035
1	Commander US Army Communications - Electronics Command ATTN: AMSEL-ED Fort Monmouth, NJ 07703
1	Commander ERADCOM Technical Library ATTN: DELSD-L (Reports Section) Fort Monmouth, NJ 07703-5301
3	Commander US Army Missile Command Research, Development & Engineering Center ATTN: AMSMI-RD Dr. B. Walker Mr. R. Deep Redstone Arsenal, AL 35898-5500
1	Director US Army Missile & Space Intelligence Center ATTN: AIAMS-YDL Redstone Arsenal, AL 35898-5500
1	Commander US Army Tank Automotive Command ATTN: AMSTA-TSL Warren, MI 48397-5500
1	Director US Army TRADOC Systems Analysis Activity ATTN: ATAA-SL White Sands Missile Range, NM 88002
1	Commander US Army Research Office P. O. Box 12211 Research Triangle Park, NC 27709

DISTRIBUTION LIST

No. of Copies	Organization
1	Commander US Naval Air Systems Command ATTN: AIR-604 Washington, D. C. 20360
2	Commander US Naval Surface Weapons Center ATTN: Dr. T. Clare, Code DK20 Dr. F. Moore Dahlgren, VA 22448-5000
1	Commander US Naval Surface Weapons Center ATTN: Dr. U. Jettmar Silver Spring, MD 20902-5000
1	Commander US Naval Weapons Center ATTN: Code 3431, Tech Lib China Lake, CA 93555
1	Commander US Army Development and Employment Agency ATTN: MODE-TED-SAB Fort Lewis, WA 98433
1	Director NASA Langley Research Center ATTN: NS-185, Tech Lib Langley Station Hampton, VA 23365
4	Director NASA Ames Research Center ATTN: MS-202-1, Dr. T. Pulliam Dr. J. Steger MS-227-8, Dr. L. Schiff Moffett Field, CA 94035
2	Commandant US Army Infantry School ATTN: ATSH-CD-CSO-OR Fort Benning, GA 31905
1	AFWL/SUL Kirtland AFB, NM 87117
1	Air Force Armament Laboratory ATTN: AFATL/DLODL Eglin AFB, FL 32542-5000
2	Director Sandia Laboratories ATTN: Division No. 1331, Dr. F. Blottner P.O. Box 580 Albuquerque, NM 87184
1	AEDC Calspan Field Services ATTN: MS 600 (Dr. John Benek) AAFS, TN 37389
1	Virginia Polytechnic Institute & State University ATTN: Dr. Clark H. Lewis Department of Aerospace & Ocean Engineering Blacksburg, VA 24061
1	University of California, Davis Department of Mechanical Engineering ATTN: Prof. H.A. Dwyer Davis, CA 95616
1	Pennsylvania State University Department of Aerospace Engineering ATTN: Dr. G. S. Dulikravich University Park, PA 16802
1	University of Florida Dept. of Engineering Sciences College of Engineering ATTN: Prof. C. C. Hsu Gainesville, FL 32611
1	University of Illinois at Urbana Champaign Department of Mechanical and Industrial Engineering ATTN: Prof. W. L. Chow Urbana, IL 61801

DISTRIBUTION LIST

No. of Copies	Organization
10	Central Intelligence Agency Office of Central Reference Dissemination Branch Room GE-47 HQS Washington, DC 20502
1	University of Maryland Department of Aerospace Engr. ATTN: Dr. J. D. Anderson, Jr. College Park, MD 20742
1	University of Notre Dame Department of Aeronautical and Mechanical Engineering ATTN: Prof. T. J. Mueller Notre Dame, IN 46556
1	University of Texas Department of Aerospace Engineering and Engineering Mechanics ATTN: Dr. D. S. Dolling Austin, Texas 78712-1055

Aberdeen Proving Ground

Dir, USAMSAA
ATTN: AMXSY-D
AMXSY-MP, H. Cohen

Cdr, USATECOM
ATTN: AMSTE-TO-F

Cdr, CRDC, AMCCOM
ATTN: SMCCR-RSP-A
SMCCR-MU
SMCCR-SPS-IL

USER EVALUATION SHEET/CHANGE OF ADDRESS

This Laboratory undertakes a continuing effort to improve the quality of the reports it publishes. Your comments/answers to the items/questions below will aid us in our efforts.

1. BRL Report Number_____ Date of Report_____

2. Date Report Received_____

3. Does this report satisfy a need? (Comment on purpose, related project, or other area of interest for which the report will be used.)_____

4. How specifically, is the report being used? (Information source, design data, procedure, source of ideas, etc.)_____

5. Has the information in this report led to any quantitative savings as far as man-hours or dollars saved, operating costs avoided or efficiencies achieved, etc? If so, please elaborate._____

6. General Comments. What do you think should be changed to improve future reports? (*Indicate changes to organization, technical content, format, etc.*)

CURRENT ADDRESS

Name

Organization

Address

City, State, Zip

7. If indicating a Change of Address or Address Correction, please provide the New or Correct Address in Block 6 above and the Old or Incorrect address below.

OLD ADDRESS

Name

Organization

Address

City, State, Zip

(Remove this sheet along the perforation, fold as indicated, staple or tape closed, and mail.)

FOLD HERE

Director
U.S. Army Ballistic Research Laboratory
ATTN: SLCBR-DD-T
Aberdeen Proving Ground, MD 21005-5066

NO POSTAGE
NECESSARY
IF MAILED
IN THE
UNITED STATES

OFFICIAL BUSINESS
PENALTY FOR PRIVATE USE, $300

BUSINESS REPLY MAIL
FIRST CLASS PERMIT NO 12062 WASHINGTON, DC

POSTAGE WILL BE PAID BY DEPARTMENT OF THE ARMY

Director
U.S. Army Ballistic Research Laboratory
ATTN: SLCBR-DD-T
Aberdeen Proving Ground, MD 21005-9989

FOLD HERE

END

DTIC

9-86